TECHNICAL MEMORANDUM

X-42

COLD-AIR INVESTIGATION OF THREE VARIABLE-THROAT-AREA CONVERGENT-DIVERGENT NOZZLES

By John E. McAulay

Lewis Research Center
Cleveland, Ohio

CLASSIFIED DOCUMENT - TITLE UNCLASSIFIED

NATIONAL AERONAUTICS AND SPACE ADMINISTRATION

WASHINGTON September 1959

NATIONAL AERONAUTICS AND SPACE ADMINISTRATION

TECHNICAL MEMORANDUM X-42

COLD-AIR INVESTIGATION OF THREE VARIABLE-THROAT-AREA CONVERGENT-DIVERGENT NOZZLES*

By John E. McAulay

SUMMARY

A program has been conducted at the NASA Lewis Research Center to evaluate methods of providing thrust modulation for solid-propellant rockets by varying the nozzle throat area. Three of these methods were evaluated in a cold-flow rig over a pressure-ratio range from 10 to 150. In one of these methods (throat injection) throat-area variation was obtained by injecting air at the nozzle throat perpendicular to the primary flow. The other two methods used physical blockage and are referred to as the throat insert and the elliptical throat.

The injection configuration produced a maximum reduction in effective nozzle throat area during the investigation of 14 percent at an injection flow ratio of 0.33 (i.e., secondary to total flow); no measurable losses in thrust ratio were evident at or near design pressure ratio. The throat-insert and the elliptical-throat configurations produced an area reduction of the order of 50 percent. For these two configurations as the nozzle throat area was reduced about 35 percent at or near design pressure ratio the thrust ratio decreased about 0.02. Larger thrust-ratio reductions were encountered at nozzle pressure ratios considerably below design.

INTRODUCTION

The thrust of solid-propellant rockets with fixed nozzles is not adjustable for variations in burning rate with grain temperature or from one propellant batch to another nor for programming. The information reported in reference 1 indicates that changing nozzle throat area is the most efficient practical method of obtaining large variations in solid-propellant rocket thrust.

In order to investigate methods of providing thrust modulation for solid-propellant rockets by varying the nozzle throat area, a research

*Title, Unclassified.

program has been conducted at the NASA Lewis Research Center. Three methods of nozzle-throat-area variation have been explored in a cold-flow rig, and the results are given herein. One method obtained area variation aerodynamically by injecting air at the nozzle throat perpendicular to the primary flow. This method as applied to convergent nozzles is discussed in reference 2. The other two methods provided throat-area variation by physical blockage of the nozzle throat. One configuration (hereinafter referred to as the throat-insert configuration) provided the blockage by introducing four rectangular flat plates in the nozzle throat perpendicular to the flow. The other blockage configuration had a nozzle throat shaped like an ellipse (referred to as the elliptical-throat configuration) and provided throat-area variation by rotating the supersonic portion of the nozzle with respect to the subsonic portion (ref. 3). All of these configurations would admittedly be more difficult to cool than a conventional nozzle. The throat-injection method, however, could be employed using a separate source of injection gas and thereby could largely eliminate any cooling problem.

Data for these three configurations were obtained over a nominal range of nozzle pressure ratios from 10 to 150. Nozzle performance data are presented to show the area variation and thrust ratio achieved. In addition, the amount of thrust modulation which might be expected with these configurations with typical solid propellants is shown.

APPARATUS

Installation

The nozzle configurations were attached to a cold-flow nozzle rig which was installed in a test chamber (fig. 1). The test chamber was connected to the altitude exhaust system. High-pressure air was supplied to the test nozzles from a duct connected to the nozzle rig by a frictionless labyrinth seal. The nozzle and its associated inlet ducting were attached rigidly to a bedplate, which was in turn supported by flexure rods. Forces on this system were transmitted to a balanced-air-diaphragm force-measuring cell. The nominal inlet and exhaust pressures available were 165 and 1.2 pounds per square inch absolute, respectively. The air temperature was approximately 540° R.

Nozzle Configurations

Throat-injection configuration. - The schematic diagram of figure 2 illustrates the main features of the throat-injection configuration. Photographs of this nozzle, which was formed from mild steel, are

presented in figure 3. As can be observed from figure 2, the secondary flow was obtained from the primary or main duct. Consequently, the magnitude of secondary flow was a function only of the size of the spacer used (fig. 2). The width of these spacers was nominally 0.10, 0.25, 0.40, or 0.55 inch. When no spacer was present, the subsonic and supersonic portions of the nozzle faired together at the nozzle throat. The variation of the area through the secondary passage (fig. 2) was such that the maximum Mach number in the inlet portion of the secondary passage was about 0.3 (i.e., assuming isentropic flow).

The geometric expansion ratio of the nozzle (figs. 2 and 3) was 7.27. This was extended to 22.7 by simply extending the divergent portion of the nozzle, the sides of which formed an included angle of 30°. The nozzle throat diameter was 4.75 inches, as was the radius of curvature of the nozzle throat. The ratio of nozzle inlet area to geometric nozzle throat area was approximately 4.

Throat-insert configuration. - The hardware used for this configuration was identical to that used for the air-injection configuration except that the spacers were replaced by a throat-insert assembly (fig. 4). Two of these assemblies were available, each having four flat plates. The flat plates of the assembly shown in figure 4 were 1 inch in width, while for the other assembly the plates were 2 inches wide. These flat plates could be moved so that the area was reduced by as much as 50 percent of its maximum area.

Elliptical-throat configuration. - The elliptical-throat nozzle was made from wood and is shown in figure 5. It was attached to the same inlet piping as the other two nozzle configurations and had nominally the same throat area when the elliptical sections matched. The throat cross section actually was not a true ellipse but essentially two semicircles whose diameters were the opposing sides of a square. The dimensions of the long and short axes were 6.32 and 3.17 inches. The maximum reduction in geometric throat area was about 44 percent. The surface connecting the elliptically shaped throat with the circular nozzle exit was formed by a series of straight lines whose average angle in relation to the nozzle centerline was about 15°. The geometric expansion ratio of this nozzle with matching throats was 7.21.

Instrumentation

Pressure and temperatures were measured at the various stations indicated in figures 1 and 2. In addition, wall static pressure taps were placed in the supersonic portion of the nozzles, 20 for the 7.27-expansion-ratio nozzle and 25 for the 22.7-expansion-ratio nozzle

(throat-injection and throat-insert configurations). The elliptical-throat nozzle had 34 wall static taps in the supersonic section of the nozzle.

PROCEDURE

For each setting of nozzle throat area given in table I approximately 18 data points were taken over a range of pressure ratios between 10 and 150 by varying the exhaust pressure. The nozzle inlet pressure and temperature were maintained at nominal values of 165 pounds per square inch absolute and 540° R.

RESULTS AND DISCUSSION

Throat-Injection Configuration

Area variation. - The flow characteristics of the throat-injection configuration are presented in figure 6. The parameters shown in this figure are, as was expected, not a function of nozzle pressure ratio, and consequently the data points plotted are an average of about 18 individual data points. In figure 6(a) the injection flow ratio (secondary to total flow) is plotted as a function of the ratio of injection slot area to geometric nozzle area. As the injection slot area was increased, the injection flow ratio increased almost linearly. The change in nozzle effective area due to the injection of secondary air is illustrated in figure 6(b), where the percent decrease in effective nozzle throat area is plotted as a function of the injection flow ratio. The effective nozzle throat area (mathematically defined in appendix B) is the area through which the total flow passes. (Symbols are defined in appendix A.) As the injection flow ratio was increased, the decrease in effective throat area became less for equal increments of injection flow ratio. At a flow ratio of 0.33 the decrease in effective area was about 14 percent.

Thrust ratio. - Thrust ratio (defined in appendix B) is presented for the air-injection nozzle configuration as a function of nozzle pressure ratio in figure 7. (Wherever it was necessary a very limited number of data points were omitted in order to keep the figures legible.) For the low-expansion-ratio nozzle (fig. 7(a)) the thrust ratio is slightly over 0.98 at design pressure ratio, and there are no measurable losses in thrust ratio due to the injection flow. For the high-expansion-ratio nozzle (fig. 7(b)) the thrust ratio is about 0.005 to 0.010 lower when injection flow is used. However, this latter nozzle was operating far below its design pressure ratio even at a pressure ratio of 125.

It might be expected that substantial losses in thrust ratio due to pressure losses would be incurred because of introducing large portions of the air perpendicular to the primary flow at the nozzle throat. However, calculations disclosed that as nozzle pressure ratio increases the thrust ratio becomes increasingly less sensitive to nozzle pressure losses. For example, at a pressure ratio of 100 the thrust ratio is reduced only 0.01 by a nozzle total-pressure loss of 15 percent.

Nozzle static-pressure distributions. - The manner in which the static pressures in the nozzle vary for the throat-injection configuration is presented in figure 8, where the local static- to total-pressure ratio is plotted as a function of distance aft of the downstream edge of the secondary injector throat. The presence of the secondary flow produced reduced pressures in the vicinity of the nozzle throat. Aside from this trend, the curves of figure 8 are quite typical of the static-pressure distribution in a convergent-divergent nozzle.

Throat-Insert Configuration

Area variation. - The nozzle-throat-area variation with the throat-insert configuration is presented in figure 9, a plot of percent decrease in effective throat area against percent decrease in geometric throat area. The data of figure 9 are for both the high- and the low-expansion-ratio nozzle as well as insert assemblies having 1- and 2-inch-wide inserts. These data exhibited no appreciable effect of either variable on the nozzle flow characteristics. The nozzle flow coefficient over the range of throat areas investigated ranged from 0.986 with the insert elements retracted to 0.870 with the minimum throat area.

Thrust ratio. - The performance of the throat-insert configuration is given in figures 10 and 11, where thrust ratio is plotted as a function of nozzle pressure ratio. Data are presented for the 1- and 2-inch inserts (figs. 10 and 11, respectively). In both figures the low-expansion-ratio data are given in part (a) and the high-expansion-ratio data are given in part (b). As throat area was reduced, the nozzle expansion ratio increased, and consequently the design pressure ratio changed as indicated in the legend.

For the low-expansion-ratio nozzle (figs. 10(a) and 11(a)), where the facility limits permitted design pressure ratio to be reached in some cases and approached in others, reducing the effective throat area by 34 percent at a given nozzle pressure ratio near its design point resulted in a maximum loss of about 0.02 in thrust ratio. At nozzle pressure ratios considerably below design the loss in thrust ratio is generally much greater (above 0.05). The greater part of these losses

at off-design conditions can be attributed to the different degree in overexpansion. The data shown in figures 10(b) and 11(b) are so far below design pressure ratio that they are only of casual interest.

A comparison of the data in figures 10 and 11 disclosed no appreciable effect on the thrust ratio due to increasing the width of the inserts from 1 to 2 inches.

Elliptical-Throat Configuration

Area variation. - As in the case of the throat-insert configuration, area variation for the elliptical-throat configuration is presented by a plot of percent decrease in effective throat area against percent decrease in geometric throat area (fig. 12). The flow coefficient of this configuration varied from 0.995 to 0.911 for an area change slightly less than that possible with the throat-insert configuration. The higher flow coefficient at maximum nozzle throat area of the elliptical nozzle (0.995) as compared with the insert nozzle (0.986) can probably be attributed to the differences in the two nozzles at the throat (i.e., contour, insert thickness, recessed volumes when insert elements are retracted).

Thrust ratio. - The performance of the elliptical-throat configuration is given in figure 13, where thrust ratio is plotted as a function of nozzle pressure ratio. With the maximum throat area the thrust ratio at nozzle pressure ratios between 80 and 120 was 0.984. Reducing the nozzle throat area by 35 percent in this pressure-ratio range resulted in a loss in thrust ratio of 0.01 to 0.02. As might have been expected, the results were very similar to those obtained with the throat-insert configuration.

Nozzle static-pressure distributions. - Typical static-pressure distributions in the supersonic portion of the elliptical-throat configuration are presented in figure 14. The low pressure in the region just downstream of the nozzle throat, where the subsonic ellipse does not match the supersonic ellipse, is due to separation of the flow around the irregularities of the throat.

Effect of Variation of Nozzle Throat Area on Thrust of Solid-Propellant Rocket

In order to give an idea of what the observed throat-area variations mean in terms of thrust modulation of a solid-propellant rocket, the curves of figure 15 are presented. These curves represent the

variation of rocket thrust with nozzle throat area. Assumptions used in obtaining these curves were constant thrust ratio and constant ideal thrust coefficient. These assumptions simplify the calculations and make the results more general without greatly affecting the answers obtained. The curves represent lines of constant propellant pressure exponent n from 0.3 to 0.5, which cover most of the current propellants. This exponent is used in the burning-rate expression $r = Kp_c^n$, where r equals the burning rate in inches per second, K is a constant which is a function of propellant temperature, p_c is the chamber pressure, and n is the pressure exponent. For the throat-injection configuration, where the throat area was reduced about 14 percent, the increase in thrust would be about 7 percent for a pressure exponent of 0.3 and 17 percent for an exponent of 0.5. The throat-insert and elliptical-throat configurations were capable of much greater amounts of area variation. For a 50-percent decrease in throat area the increase in thrust would range from 34 to 100 percent as the pressure exponent was varied from 0.3 to 0.5.

CONCLUDING REMARKS

A cold-flow investigation was made of three methods of obtaining thrust modulation for solid-propellant rockets by variation of nozzle throat area. For the throat-injection configuration the maximum effective area reduction obtained was 14 percent. This variation in area was accomplished with no loss in thrust ratio at or near design pressure ratio. Nozzle-throat-area variations of the order of 50 percent were obtained for the particular throat-insert and elliptical-throat configurations investigated. Of course, for these types of configurations larger variations in throat area are possible. For these latter two configurations the loss in thrust ratio at or near design pressure ratio was 0.02 or less for an area reduction of about 35 percent. Larger penalties were incurred at nozzle pressure ratios considerably below design.

The effect of nozzle-throat-area variation on rocket thrust is such that a 14-percent reduction in throat area increases the thrust from 7 to 17 percent as the propellant pressure exponent is varied from 0.3 to 0.5. For the same range in exponent a 50-percent reduction in throat area results in a thrust increase from 34 to 100 percent.

Lewis Research Center
National Aeronautics and Space Administration
Cleveland, Ohio, April 28, 1959

APPENDIX A

SYMBOLS

A	area, sq ft
B	thrust scale force, lb
C_d	flow coefficient
C_F	thrust coefficient
F	thrust, lb
$\frac{F}{F_{id}}$	thrust ratio
g	acceleration due to gravity, 32.17 ft/sec^2
M	Mach number
P	total pressure, lb/sq ft abs
p	static pressure, lb/sq ft abs
R	gas constant, 53.4 ft-lb/(lb)($^\circ$R)
T	total temperature, $^\circ$R
V	velocity, ft/sec
w_a	airflow, lb/sec
γ	ratio of specific heats
δ	ratio of total pressure to static pressure of NACA standard atmosphere at sea level
θ	ratio of total temperature to static temperature of NACA standard atmosphere at sea level

Subscripts:

ac	actual
eff	effective

i	injection airflow measuring station
id	ideal
link	thrust member
s	secondary
seal	labyrinth seal
t	total
th	nozzle throat
x	constant-area inlet duct to Venturi meter
0	exhaust or free stream
1	airflow measuring station, Venturi meter
2	nozzle inlet

APPENDIX B

METHODS OF CALCULATION

Airflow

The total airflow was calculated at a Venturi measuring station as follows:

$$w_{a,1} = C_{d,1} p_1 A_1 \sqrt{\frac{2\gamma_1 g}{(\gamma_1 - 1)RT_1}\left(\frac{P_1}{p_1}\right)^{\frac{\gamma_1 - 1}{\gamma_1}}\left[\left(\frac{P_1}{p_1}\right)^{\frac{\gamma_1 - 1}{\gamma_1}} - 1\right]} \qquad (1)$$

where

$$C_{d,1} = 0.984$$

The nozzle-throat-injection airflow was calculated using equation (1) and the total and static pressures of the injection passage, that is, P_i and p_i, and $C_{d,i} = 0.95$.

The ideal nozzle airflow was calculated as follows except with injection flow:

$$w_{a,th} = \sqrt{\frac{\gamma_1 g}{R}} \frac{A_{th} P_2}{\sqrt{T_1}} \frac{M_{th}}{\left(1 + \frac{\gamma - 1}{2} M_{th}^2\right)^{\frac{\gamma_1 + 1}{2(\gamma_1 - 1)}}} \qquad (2)$$

where for air at sonic velocity

$$\frac{M_{th}}{\left(1 + \frac{\gamma - 1}{2} M_{th}^2\right)^{\frac{\gamma_1 + 1}{2(\gamma_1 - 1)}}} = 0.5786$$

Nozzle throat flow coefficient. - The nozzle throat flow coefficient was calculated except with injection flow as follows:

$$C_{d,th} = \frac{w_{a,1}}{w_{a,th}} \qquad (3)$$

Effective nozzle throat area. - When the injection flow was zero, the nozzle throat effective area was obtained from the following expression:

$$A_{th,eff} = A_{th}C_{d,th} \tag{4}$$

When the injection flow was greater than zero,

$$(A_{th,eff})_{w_{a,i}>0} = (A_{th,eff})_{w_{a,i}=0} \left(\frac{w_{a,1}\sqrt{\theta_1}}{\delta_2}\right)_{w_{a,i}>0} \Bigg/ \left(\frac{w_{a,1}\sqrt{\theta_1}}{\delta_2}\right)_{w_{a,i}=0} \tag{5}$$

Thrust. - The nozzle jet thrust was determined from the following equation:

$$F = B + A_{seal}(P_1 - p_0) + A_{link}(2050 - p_0) + \frac{w_{a,1}}{g} V_x \tag{6}$$

Actual thrust coefficient. - The actual thrust coefficient was defined as:

$$C_{F,ac} = \frac{F}{A_{th,eff}P_2} \tag{7}$$

Ideal thrust coefficient. - The ideal thrust coefficient was determined as follows:

$$C_{F,id} = \left(\frac{w_a\sqrt{\frac{R}{g}T}}{PA_{th,eff}}\right)\left(\frac{V_{id}}{\sqrt{gRT}}\right) \tag{8}$$

where for air at sonic velocity

$$\frac{w_a\sqrt{R/gT}}{PA_{th,eff}} = 0.6846$$

and

$$\frac{V_{id}}{\sqrt{gRT}} = \sqrt{\frac{2\gamma_1}{\gamma_1 - 1}\left(\frac{p_0}{P_2}\right)^{\frac{\gamma_1-1}{\gamma_1}}\left[\left(\frac{P_2}{p_0}\right)^{\frac{\gamma_1-1}{\gamma_1}} - 1\right]}$$

Thrust ratio. - The thrust ratio was defined as

$$\frac{F}{F_{id}} = \frac{C_{F,ac}}{C_{F,id}} \tag{9}$$

REFERENCES

1. Kramer, Fritz: On Thrust Control of Solid-Propellant Motors. Rep. 6M99, Redstone Arsenal, May 1, 1957.

2. McArdle, Jack G.: Internal Characteristics and Performance of an Aerodynamically Controlled, Variable-Discharge Convergent Nozzle. NASA TN 4312, 1958.

3. Latimer, Lawrence E.: Static Tests of Three MK4 Mod 2 Jatos with Variable Nozzle Throat Area Mechanism. Rep. 3M120P, Redstone Arsenal, Aug. 15, 1957.

TABLE I. - RANGE OF PRIMARY INDEPENDENT VARIABLES

Nominal expansion ratio	Throat injection slot width, in.
Throat-injection configuration	
7.27 ↓ 22.7 ↓	0 .106 .257 .406 .556 0 .106 .257 .406 .556
Nominal expansion ratio	**Measured or geometric throat area, sq ft**
Throat-insert configuration, 1-inch inserts	
7.27 ↓ 22.7 ↓	0.123 .111 .099 .087 .123 .111 .099 .087 .078 .071
Throat-insert configuration, 2-inch inserts	
7.27 ↓ 22.7 ↓	0.123 .111 .099 .087 .123 .111 .099 .087 .074 .061
Elliptical-throat configuration	
7.21 ↓	0.124 .111 .098 .087 .078 .070

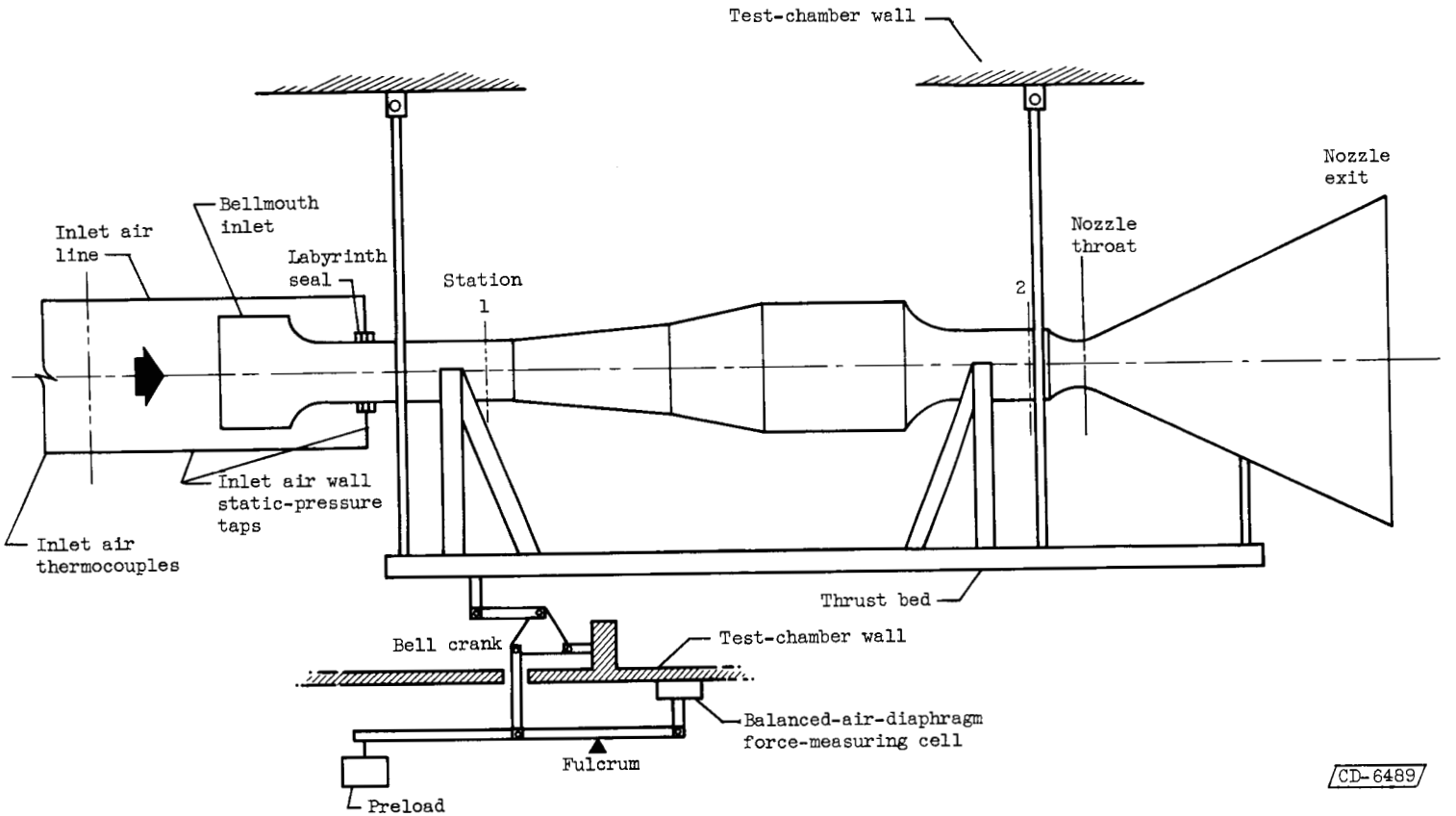

Station	Number of Probes			Number of boundary-layer rakes
	Total pressure	Wall static pressure	Thermocouples	
Inlet air	-	8	11	-
Bellmouth inlet	-	5	-	-
1	12	6	-	3
2	20	6	10	1
Ambient	-	4	-	-

Figure 1. - Schematic diagram of nozzle test rig showing instrumentation location.

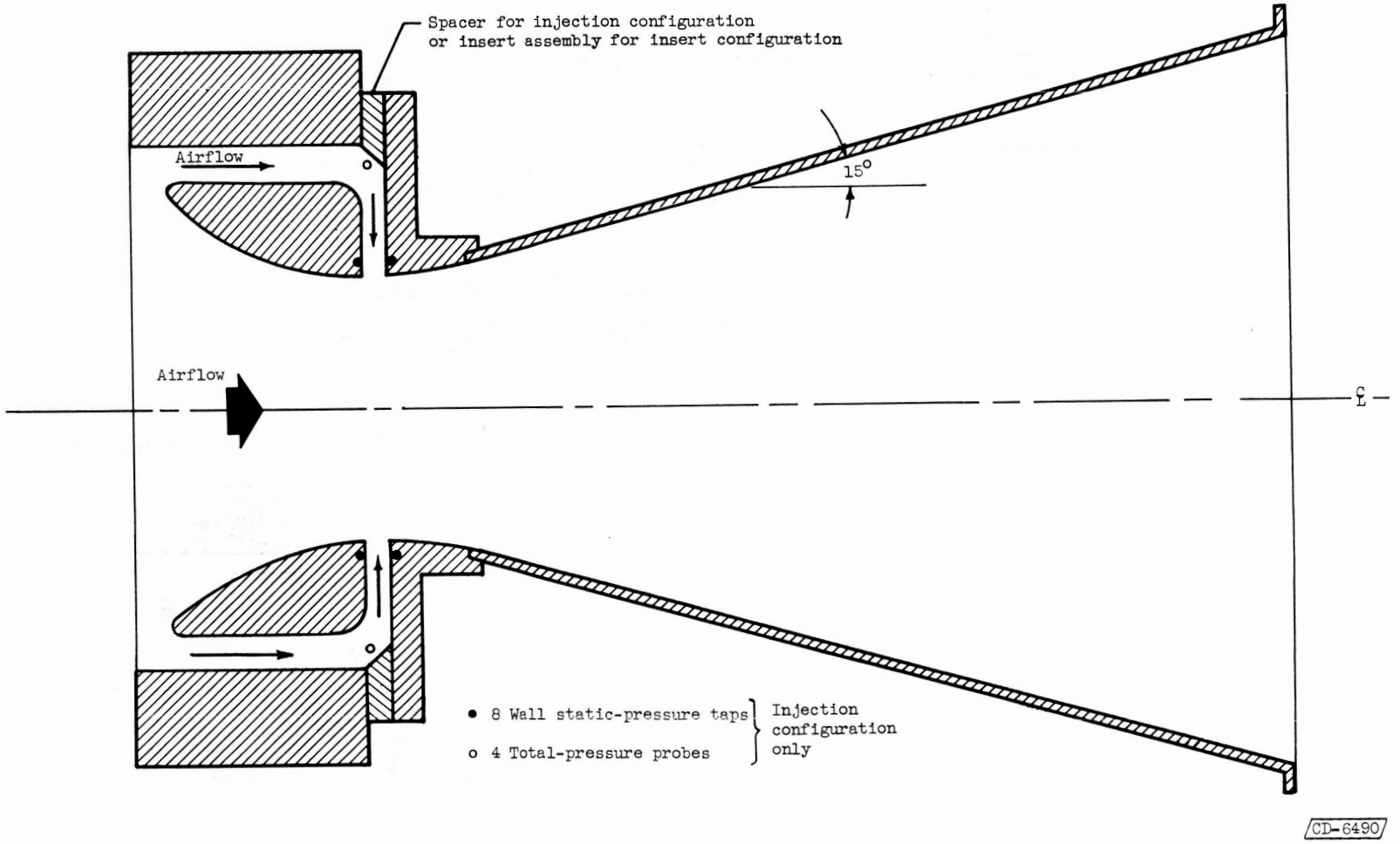

Figure 2. - Schematic cross section of low-expansion-ratio nozzle (throat-injection and throat-insert configurations).

(a) Supersonic portion of nozzle.

Figure 3. - Throat-injection configuration.

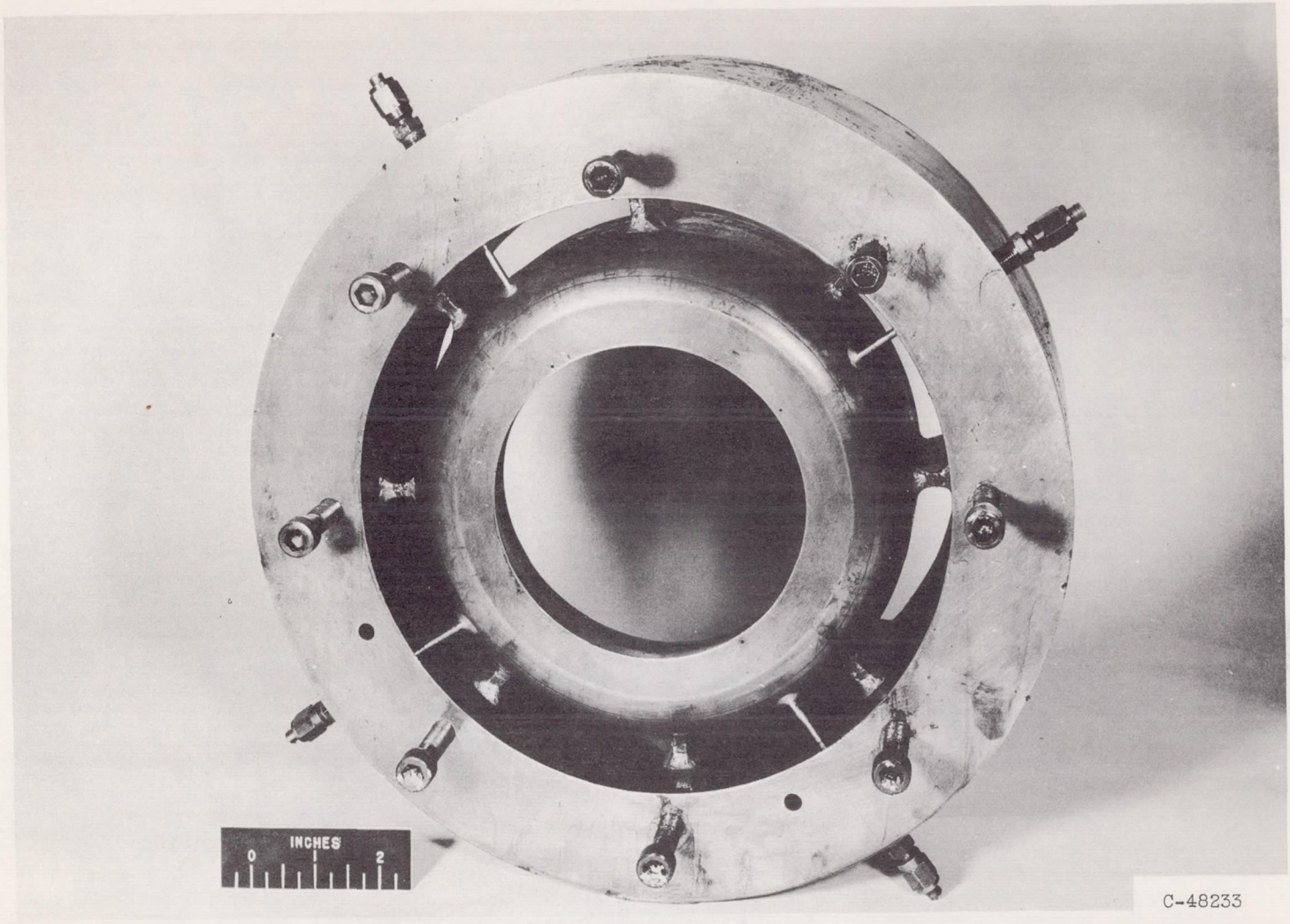

(b) Subsonic portion of nozzle.

Figure 3. - Continued. Throat-injection configuration.

(c) Assembled nozzle.

Figure 3. - Concluded. Throat-injection configuration.

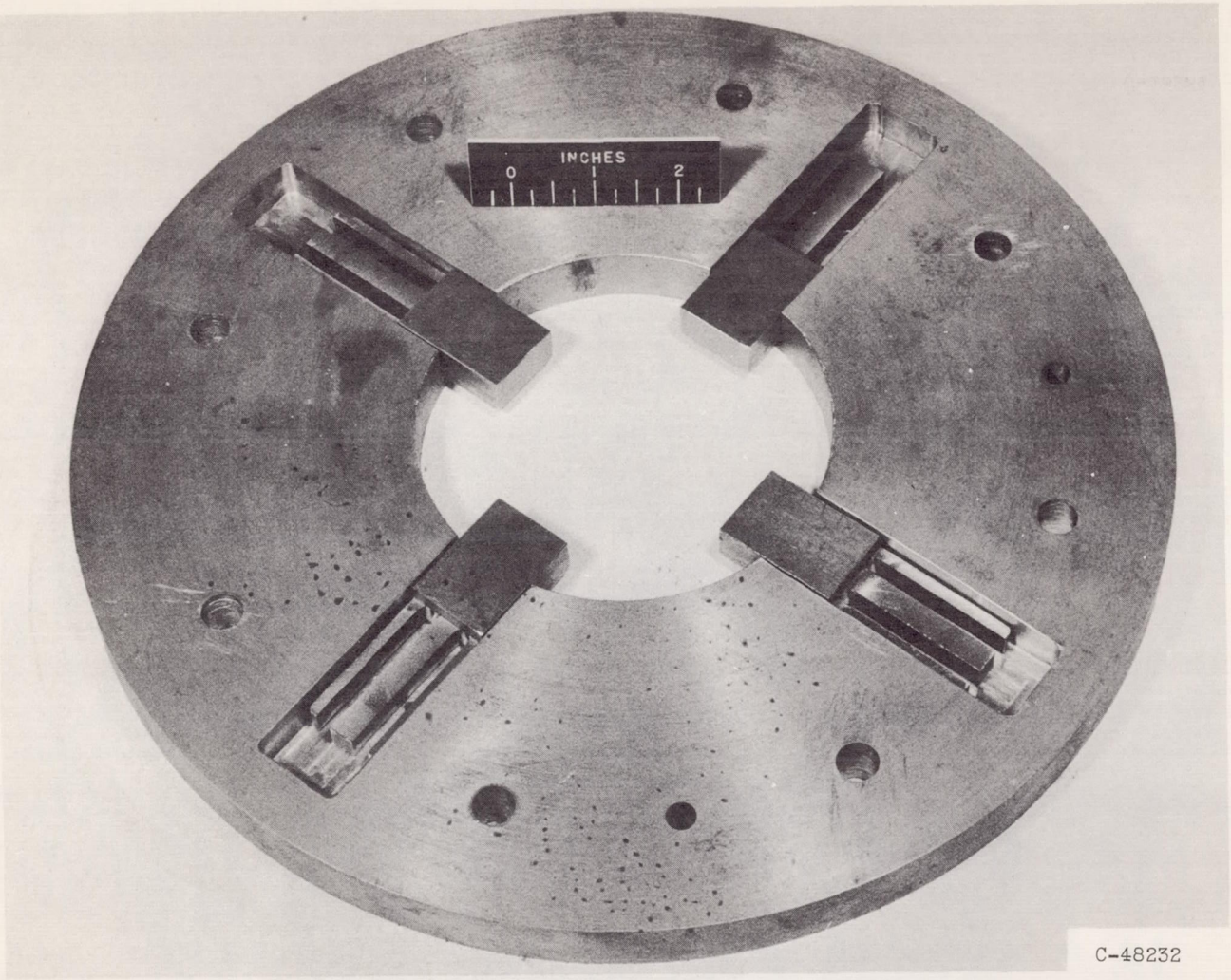

Figure 4. - Throat-insert assembly for throat-insert configuration.

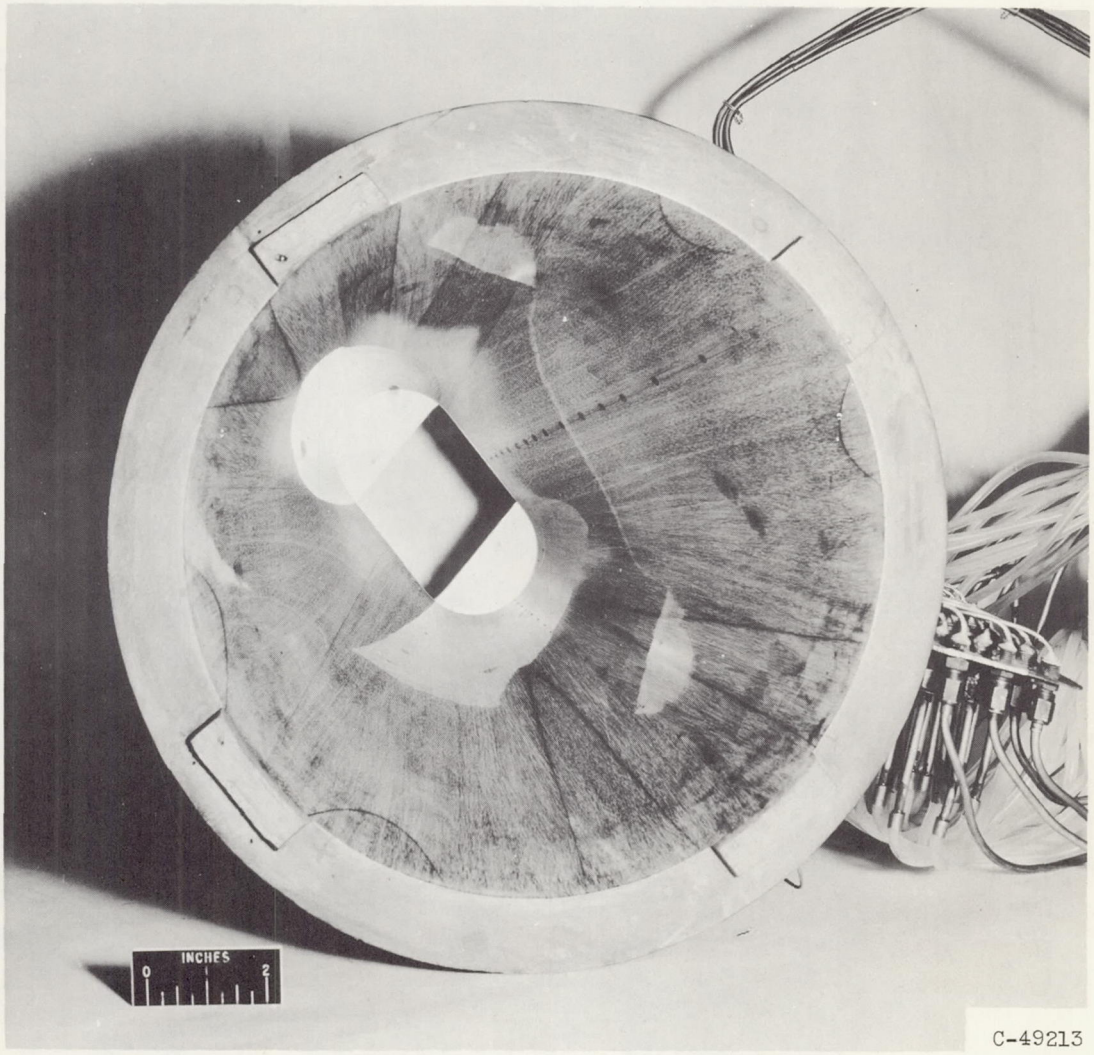

(a) Supersonic portion of nozzle.

Figure 5. - Elliptical-throat configuration.

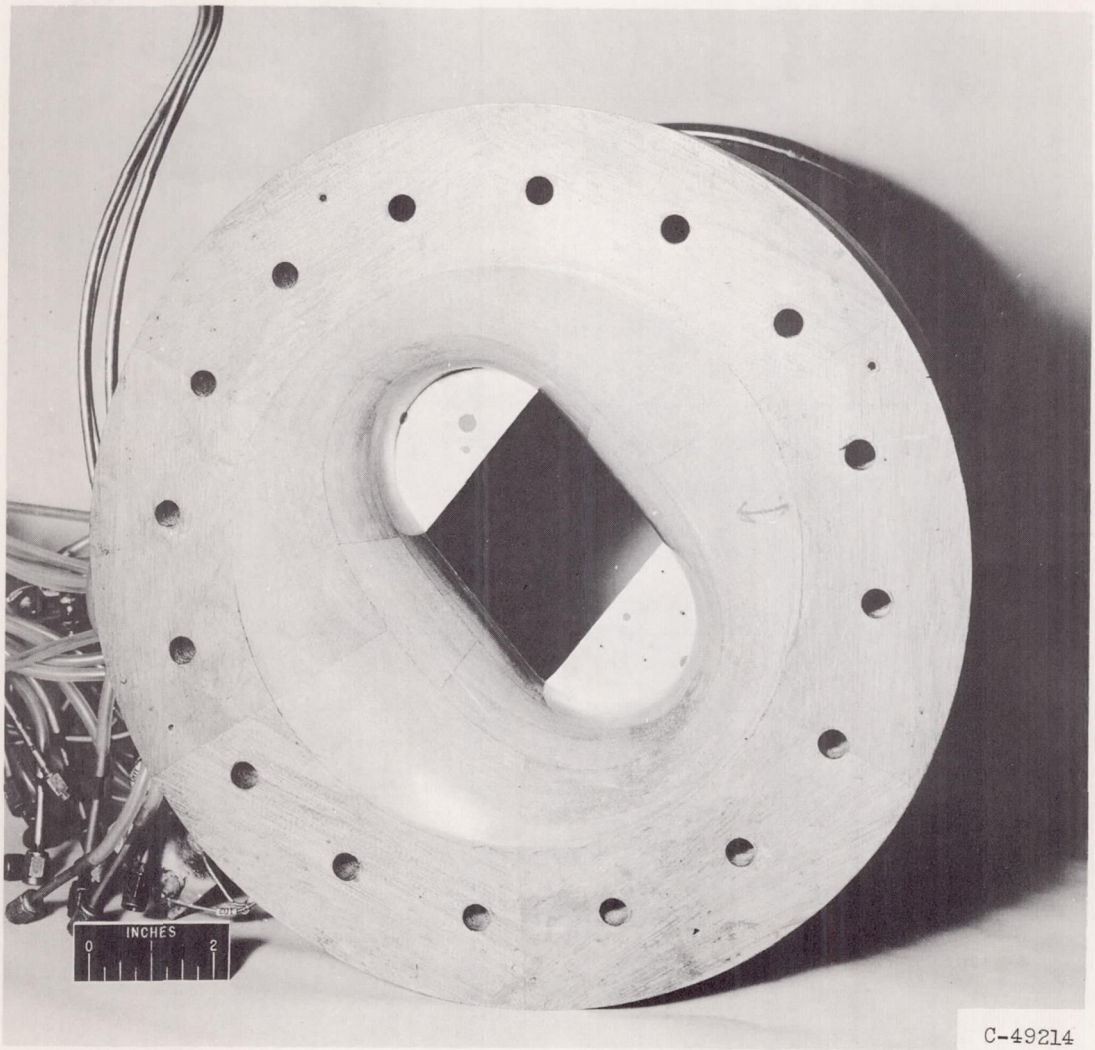

(b) Subsonic portion of nozzle.

Figure 5. - Concluded. Elliptical-throat configuration.

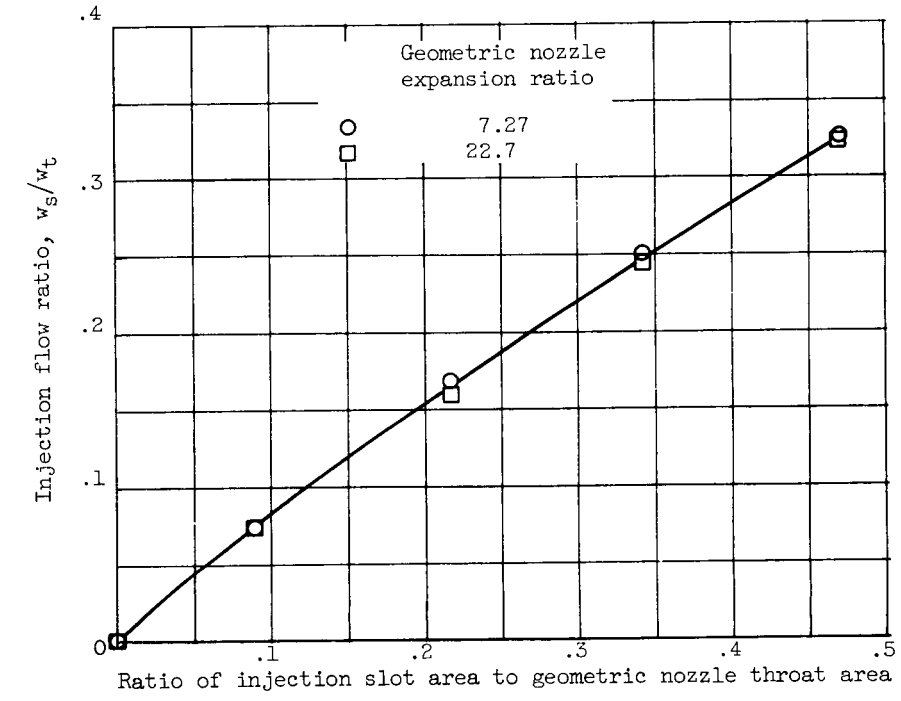

(a) Variation of injection flow ratio with injection slot area.

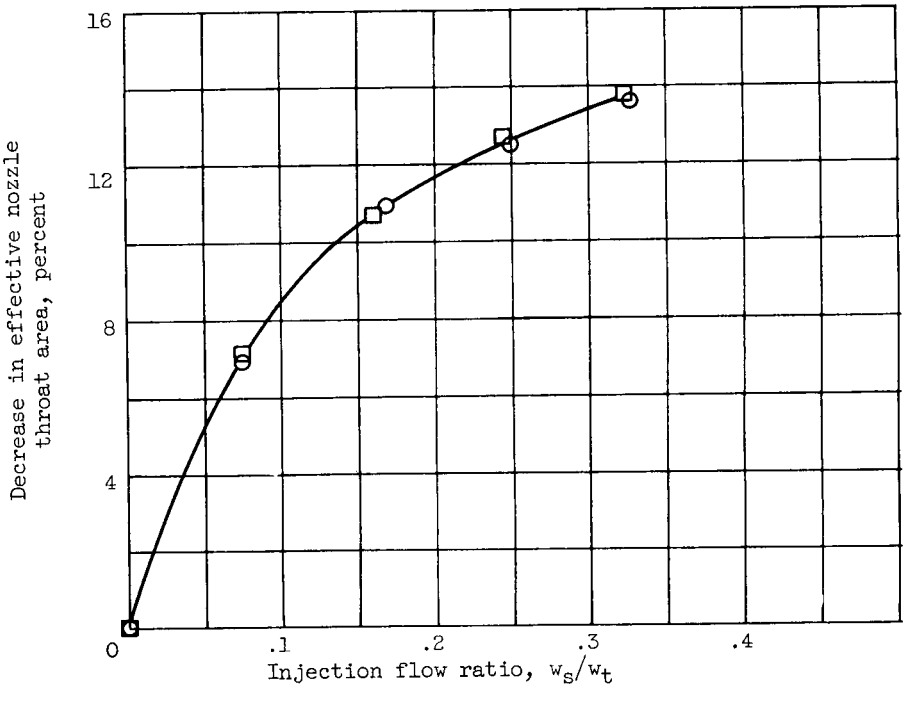

(b) Variation of effective nozzle throat area with injection flow ratio.

Figure 6. - Flow characteristics of throat-injection configuration.

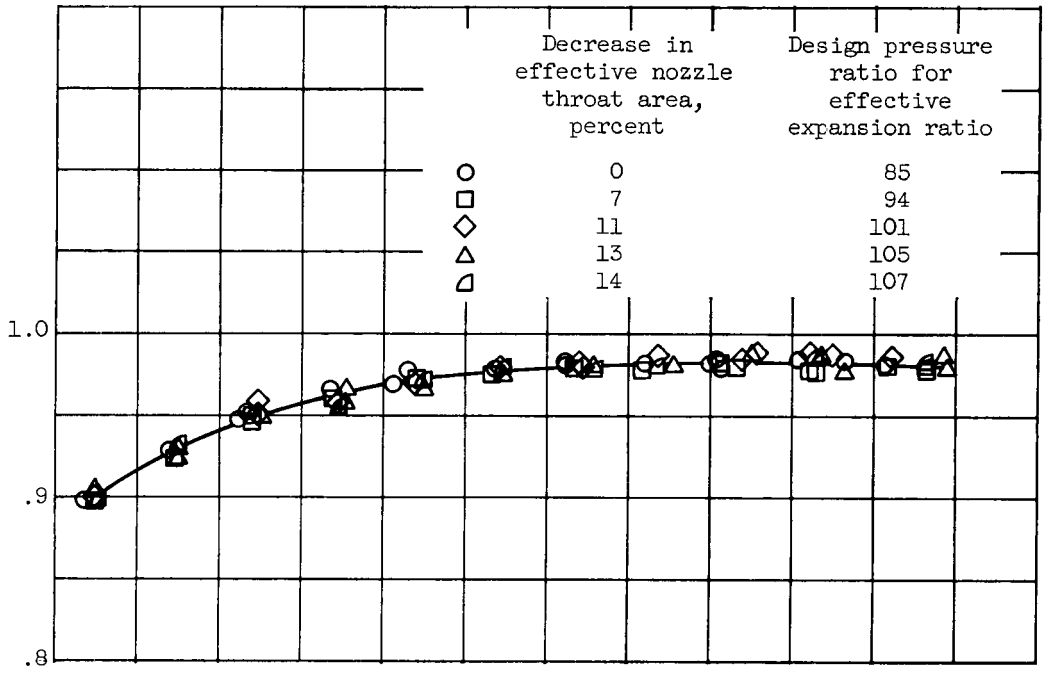

(a) Geometric nozzle expansion ratio, 7.27.

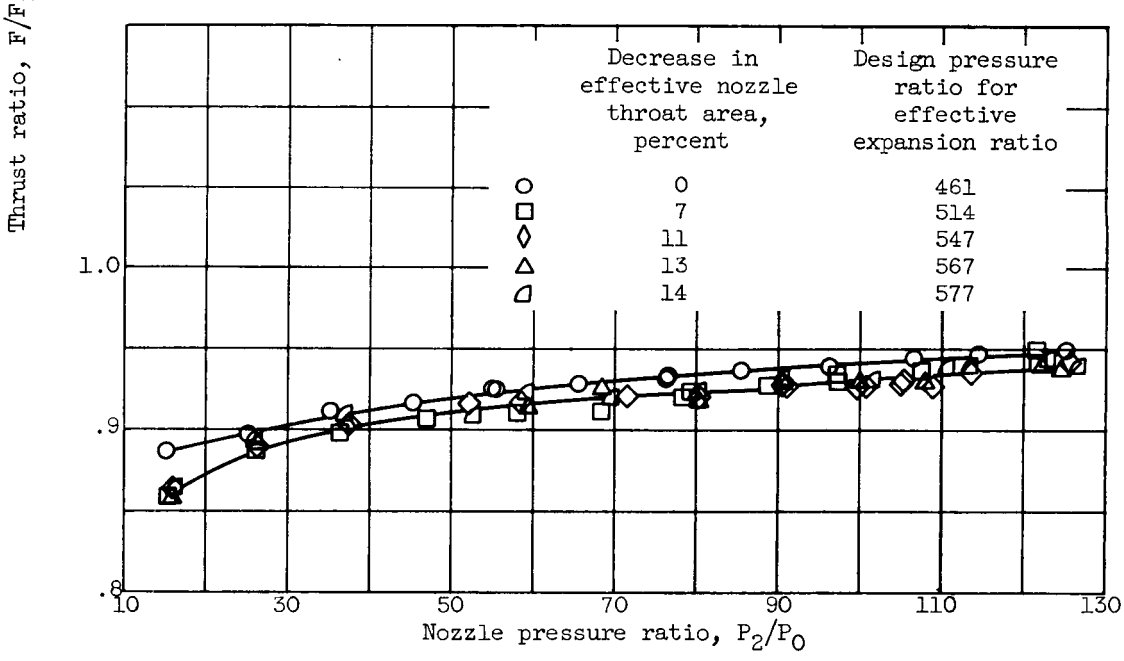

(b) Geometric nozzle expansion ratio, 22.7.

Figure 7. - Performance of throat-injection configuration.

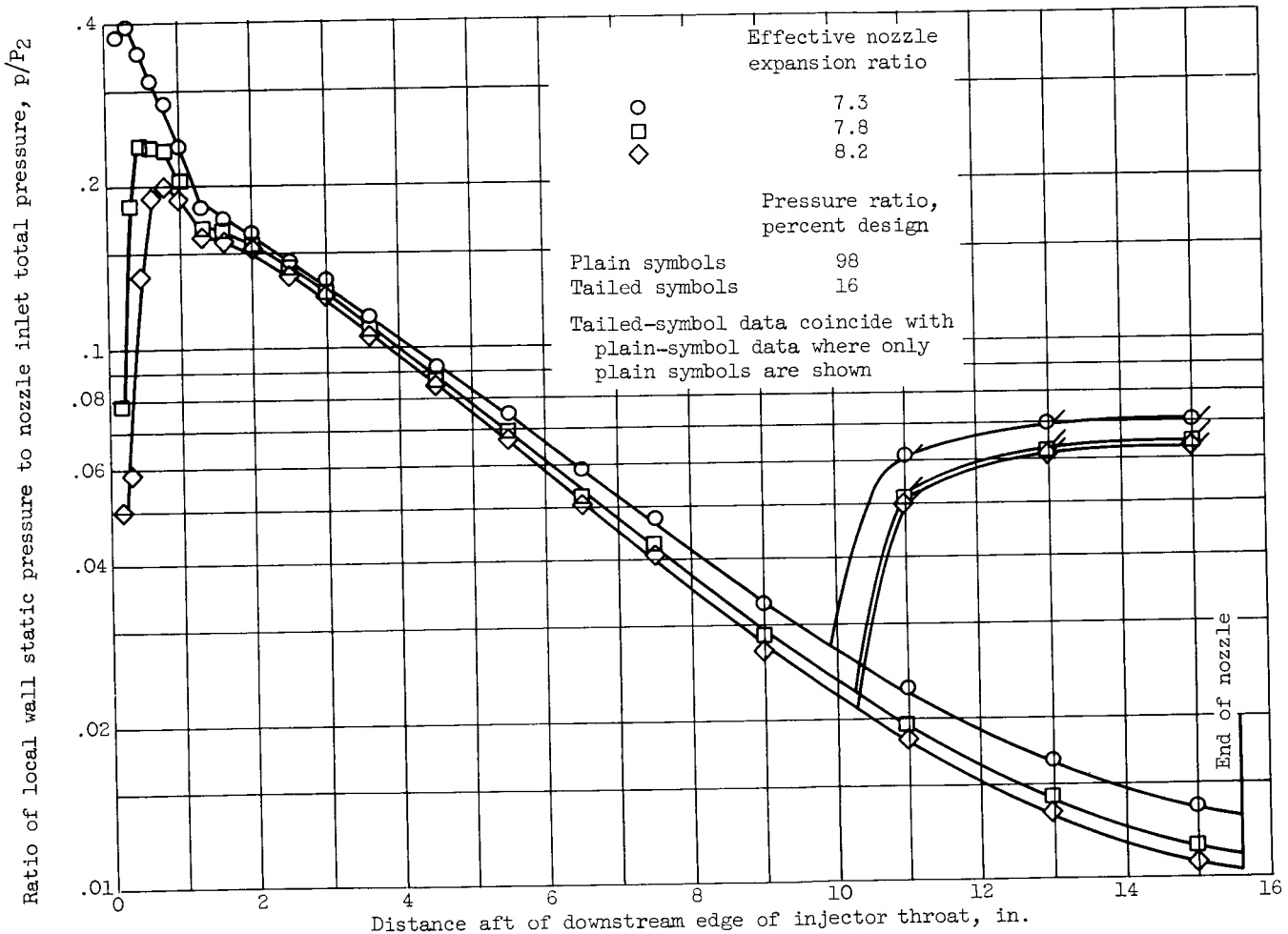

(a) Geometric nozzle expansion ratio, 7.27. (Data for effective expansion ratios above 8.2 do not materially differ from 8.2 data.)

Figure 8. - Typical nozzle pressure distributions for throat-injection configuration.

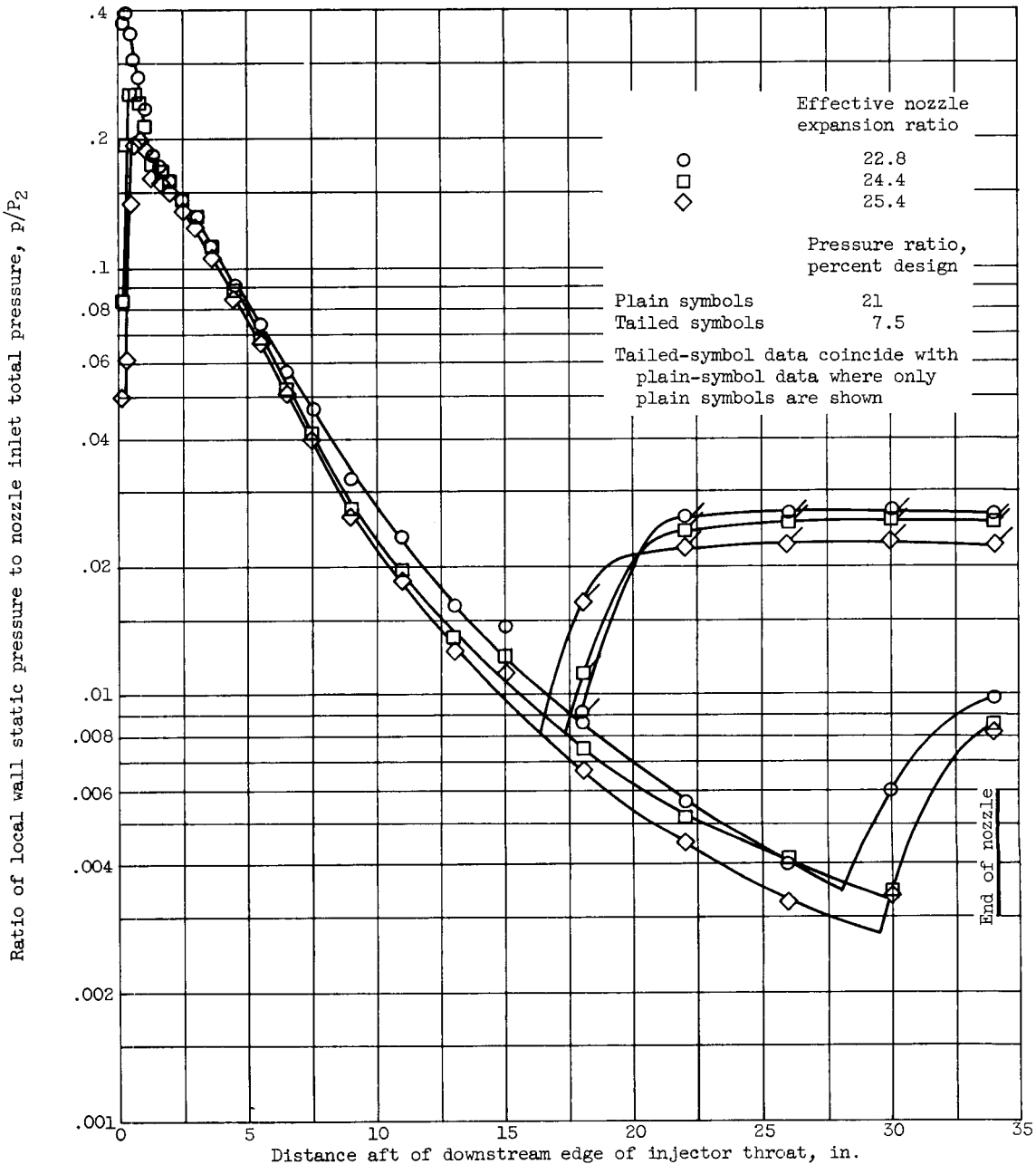

(b) Geometric nozzle expansion ratio, 22.7. (Data for effective nozzle ratios above 25.4 do not materially differ from 25.4 data.)

Figure 8. - Concluded. Typical nozzle pressure distributions for throat-injection configuration.

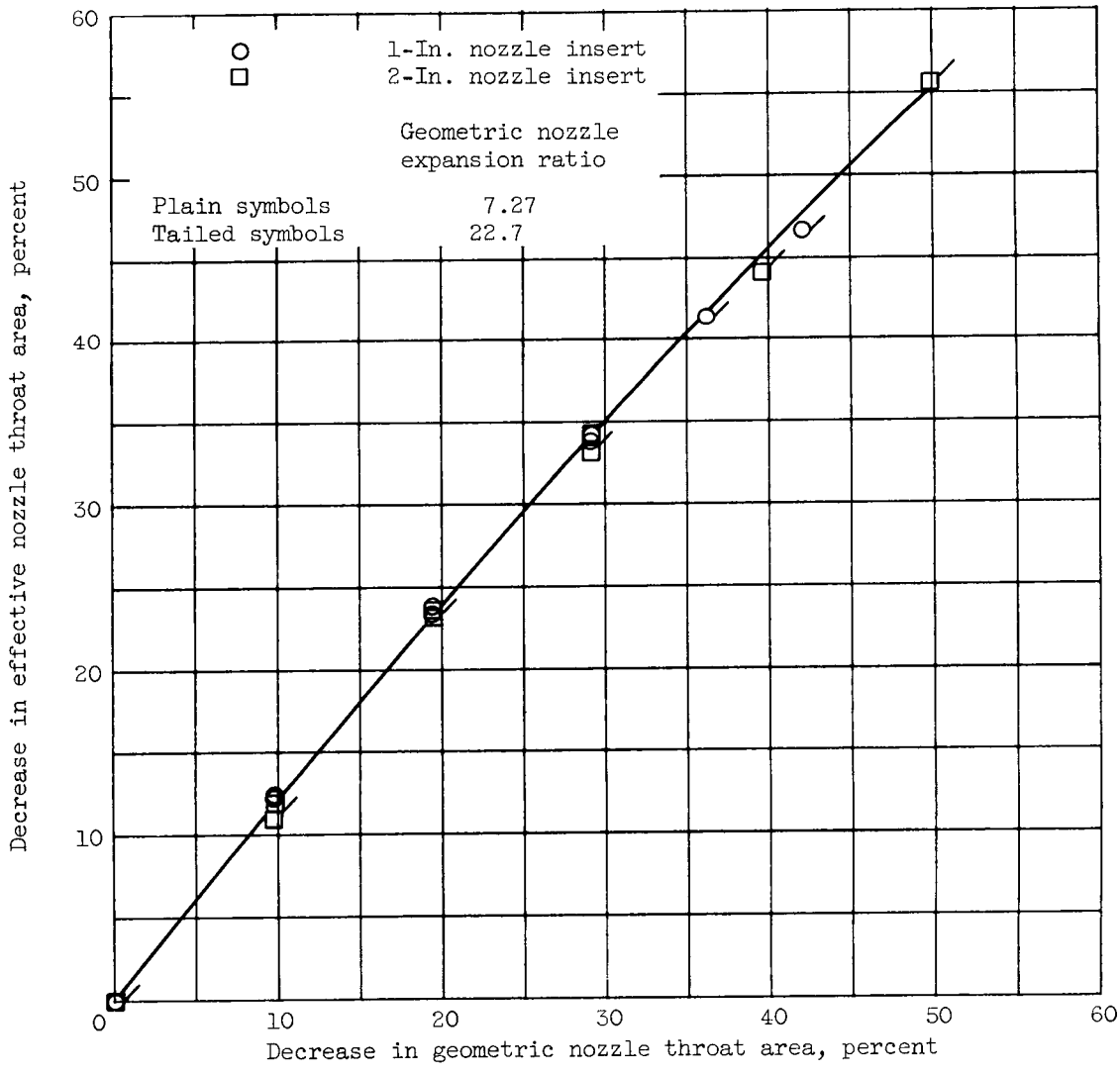

Figure 9. - Flow characteristics of throat-insert configurations.

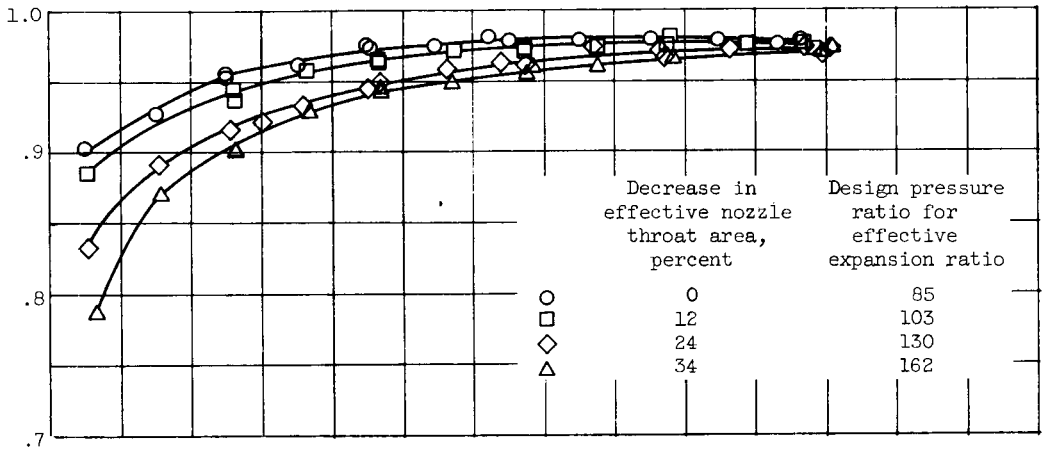

(a) Basic geometric nozzle expansion ratio, 7.27.

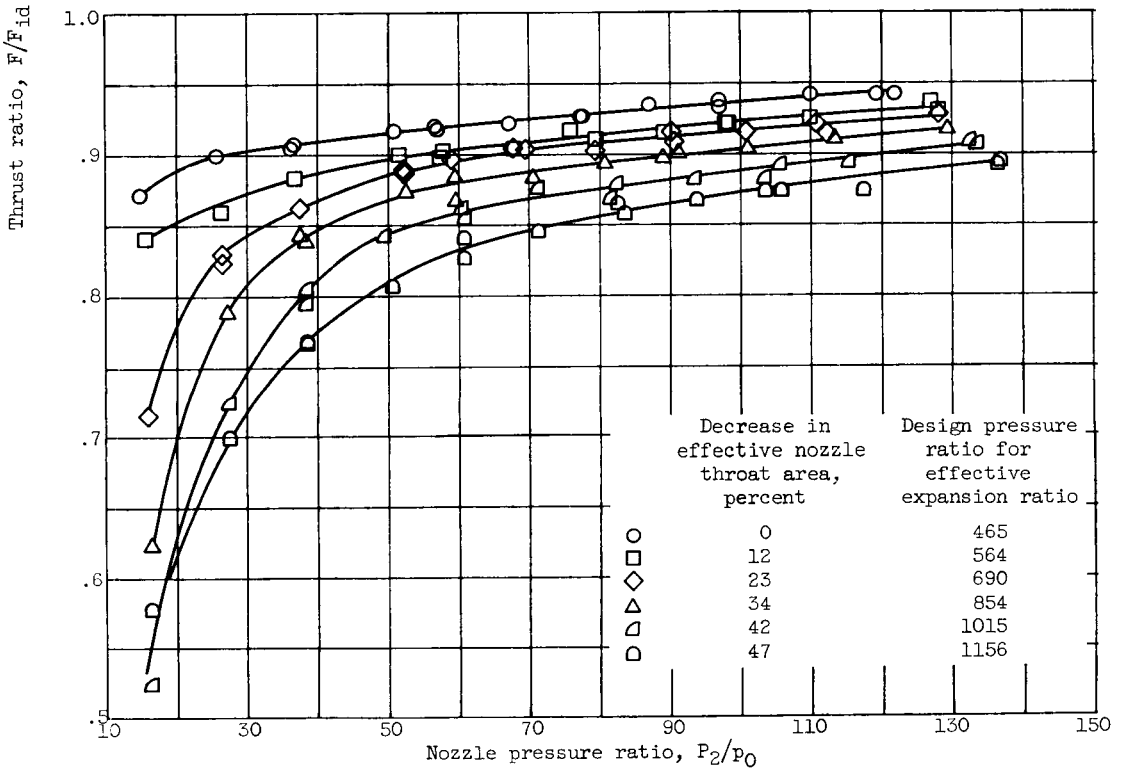

(b) Basic geometric nozzle expansion ratio, 22.7.

Figure 10. - Performance of throat-insert configuration with 1-inch nozzle insert.

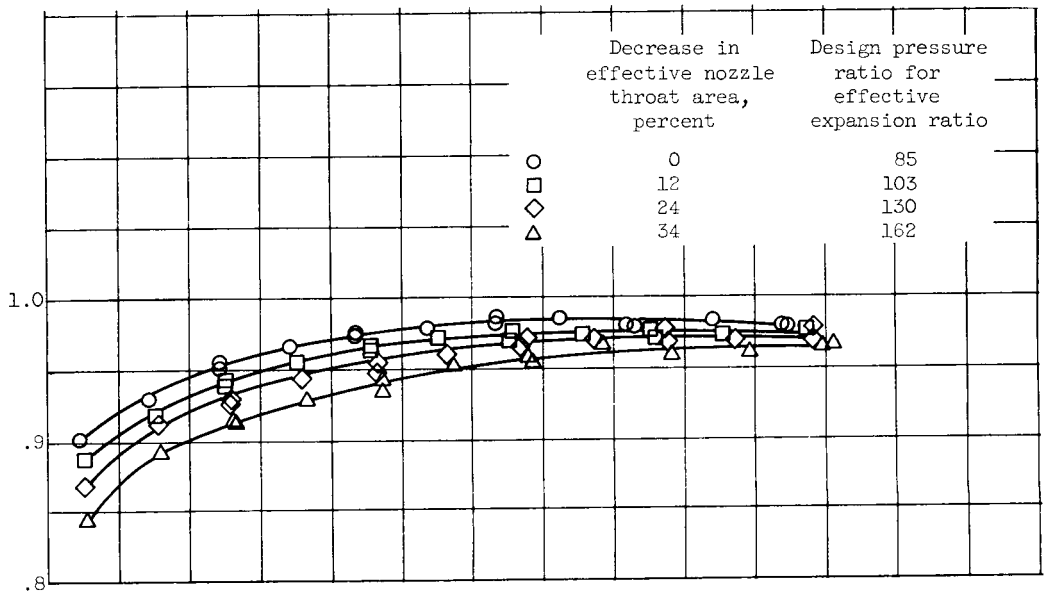

(a) Basic geometric nozzle expansion ratio, 7.27.

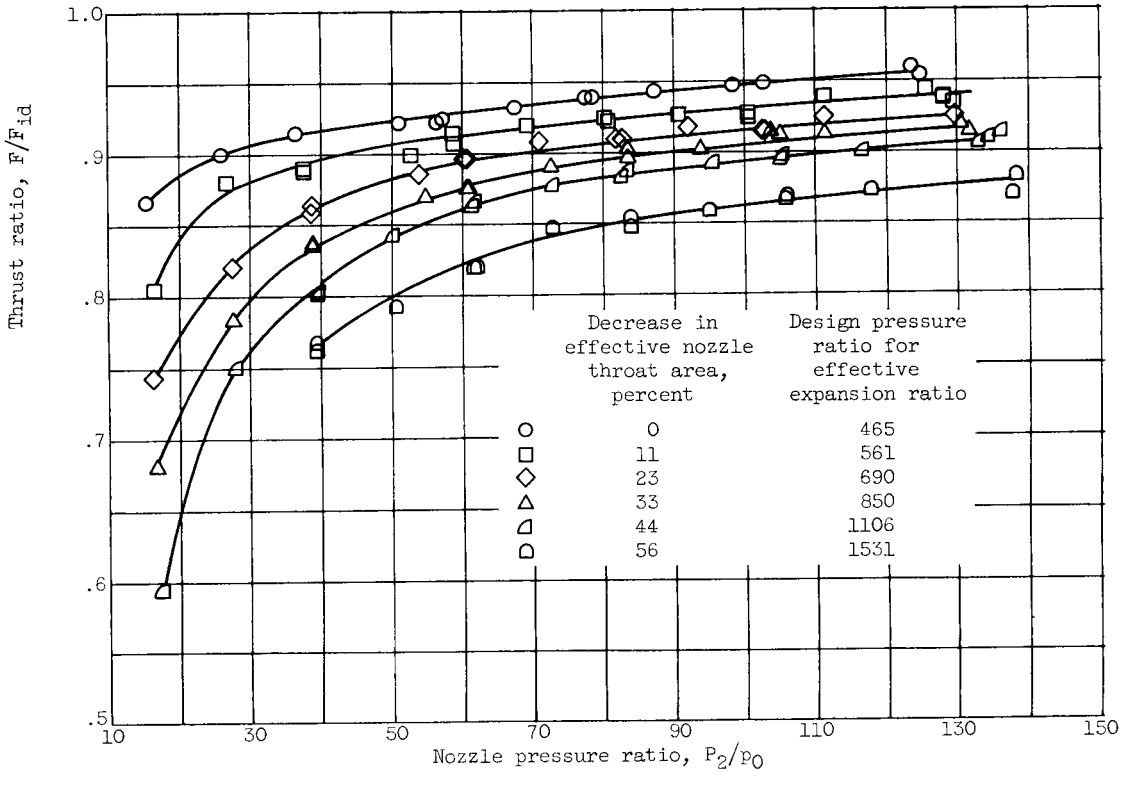

(b) Basic geometric nozzle expansion ratio, 22.7.

Figure 11. - Performance of throat-insert configuration with 2-inch nozzle insert.

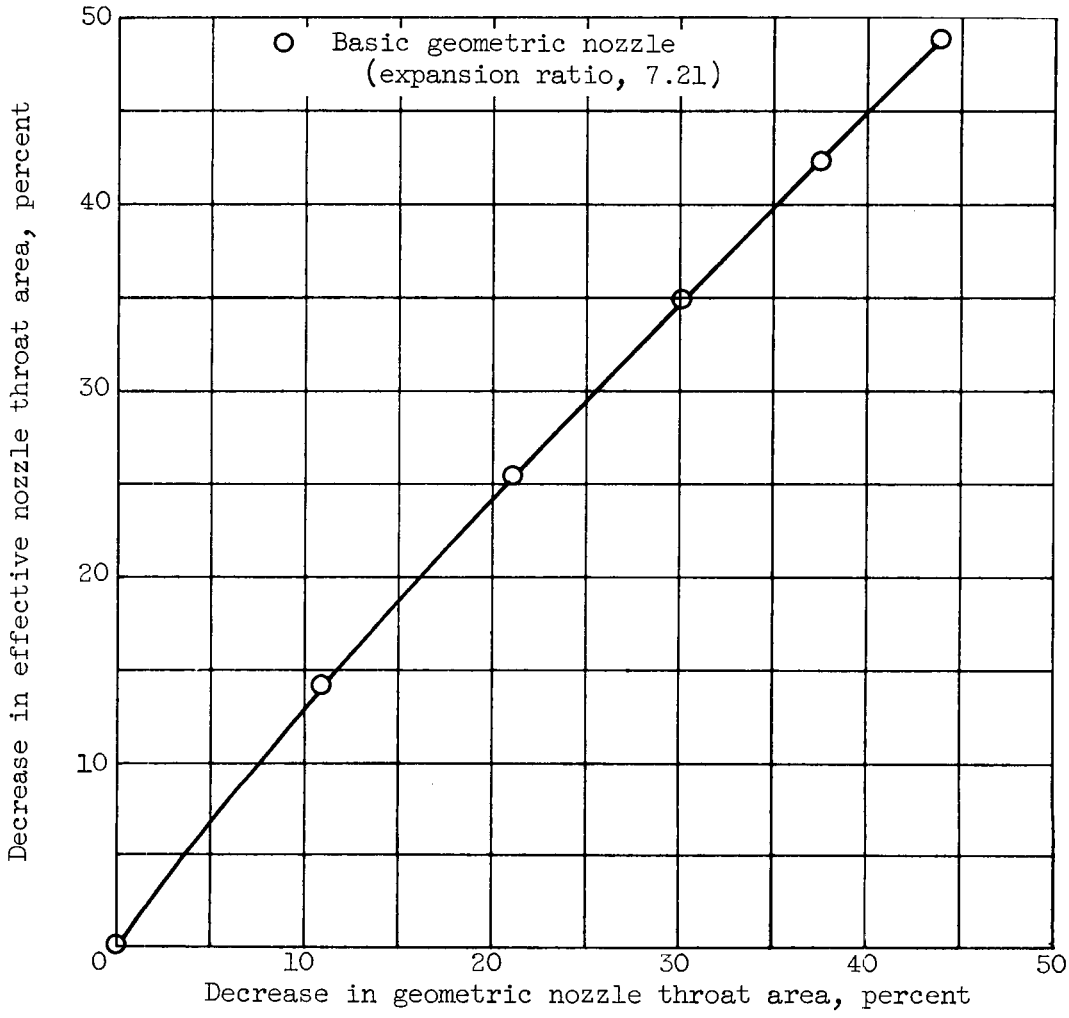

Figure 12. - Flow characteristics of elliptical-throat configuration.

Figure 13. - Performance of elliptical-throat configuration.

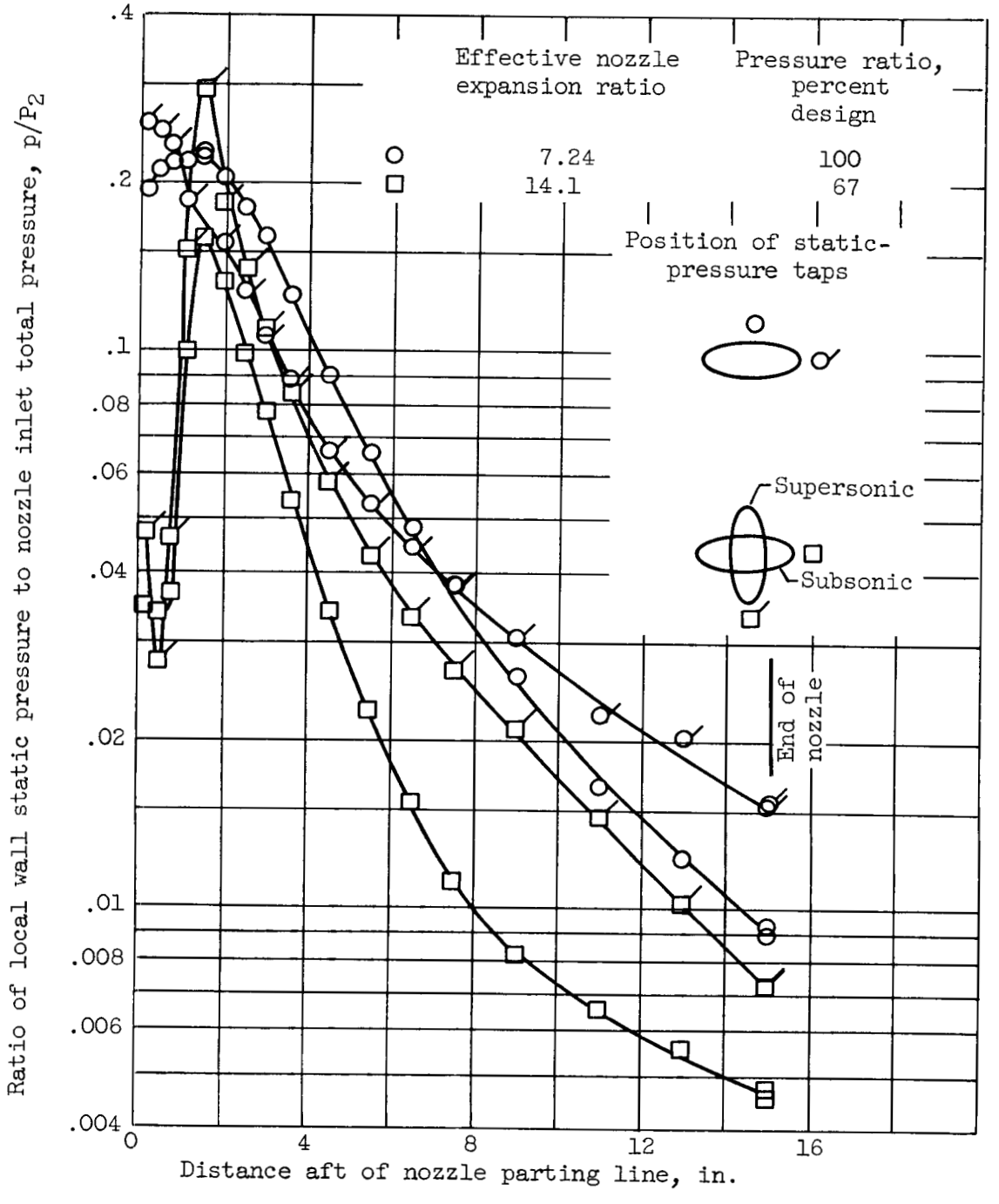

Figure 14. - Typical nozzle pressure distribution for elliptical-throat configuration.

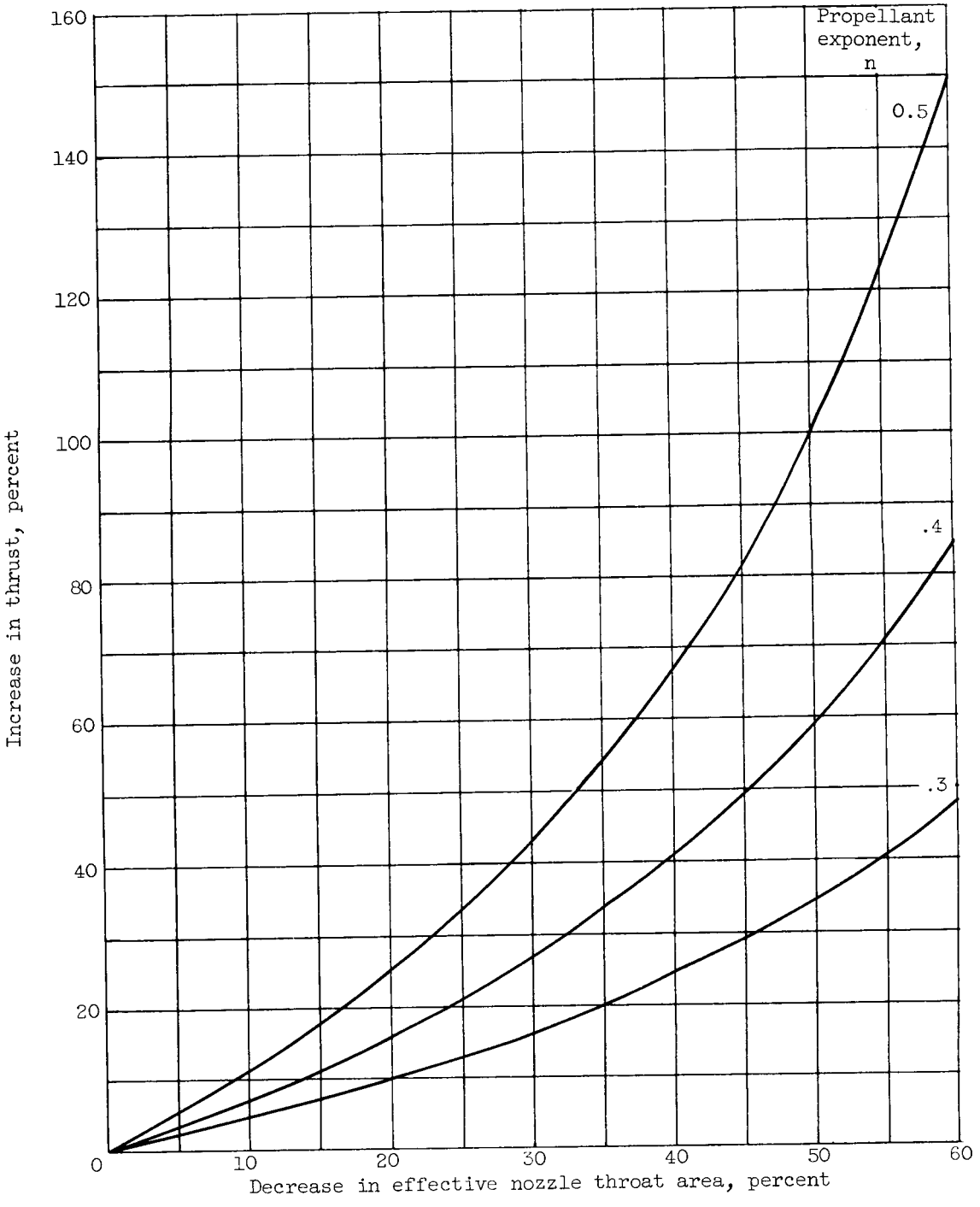

Figure 15. - Effect of nozzle-throat-area variation on thrust of solid-propellant rocket. Thrust ratio and ideal thrust coefficient assumed constant.